POAC'23
Glasgow, United Kingdom

Proceedings of the 27th International Conference on
Port and Ocean Engineering under Arctic Conditions
12-16 June 2023, Glasgow, United Kingdom

Design-purpose Numerical Simulations of the NRC Heavy Impact Test Theater (HITT)

Robert Gagnon[1], Bruce Quinton[2], John Mackay[3], Ian Robbins[1], Mark Rodriguez[4]

[1] National Research Council Canada (NRC), St. John's, Canada; [2] Memorial University of Newfoundland (MUN), St. John's, Canada);
[3] Defense Research and Development Canada (DRDC), Dartmouth, Canada; [4] Naval Surface Warfare Center (NSWC) Carderock Division, Bethesda, USA

ABSTRACT

The National Research Council of Canada, with its collaborating partners (Defence Research and Development Canada and the US Navy), are developing a new facility, known as the Heavy Impact Test Theater (HITT), that will be part of the Ice Tank facility at the NRC St. John's location. This facility will enable full-scale, or near full-scale, ice / ship-grillage impact experiments in water, where damage would be imposed on the grillage. Here we present results from sufficiently elaborate numerical simulations intended to assist with the design of HITT. In general, the simulations include representations of the moving Ice Tank carriage and the large flooded impacting device (known as the 'Hammer'), which hangs from the carriage on four chains/cables. When impact is involved, the simulations also include the hybrid ice / flooded-structure component (known as the Anvil). The simulations are useful for predicting starting and stopping loads on the carriage, lateral side loads on the carriage during the ice impact events, and formulating load-mitigating strategies where necessary. An underlying purpose of the simulations was to investigate the reliability of the simulation results when compared to actual half-scale HITT experiments (not involving impact) that were performed in NRC's Large Towing Tank. Additionally, full-scale HITT simulations were conducted showing anticipated displacement and load behaviors associated with the Hammer impacting the Anvil. The simulations involving impact incorporate NRC's validated crushable-foam ice model.

KEY WORDS: Ice impact; Grillage deformation; Design simulations; Laboratory tests.

INTRODUCTION

Marine transportation in Arctic regions is seriously affected by the presence of glacial and sea ice masses. Of concern for ships (including naval vessels) are bergy bits and growlers

(house-sized and car-sized glacial ice masses) and sea ice masses (e.g. a chunk of multi-year sea ice, a chunk from a dense sea ice rubble field or from a consolidated ridge, individual floes or smaller portions broken from floes). Detection of ice masses is sometimes difficult using marine radar in rough sea states. These considerations relate to Arctic and lower-latitude cold-water activities, such as resource development, transportation, tourism, sovereignty/security issues and environmental monitoring. Should ice make contact with a ship's hull, the impact forces will depend on the masses of the vessel and ice, the hydrodynamics of the interaction, the ship structure, the shape of the ice mass and its local crushing properties. NRC has been studying various aspects of the problem for several years, with the overall objective of creating a validated numerical model of ship/ice collisions using LS-Dyna™ software. Others have been specifically studying grillage damage associated with ice interaction for many years (e.g. Daley et al., 2007; Kõrgesaar et al., 2018).

To facilitate a critical aspect of the simulations, i.e. validation, NRC is collaborating with DRDC and the US Navy to conduct ice impact tests of naval vessel hull structures in the NRC Ice Tank in St. John's, NL. This will involve using heavy-mass flooded structures for the ship hulls and large hybrid ice-structure masses to generate significant impact loads. The planned facility, known as the Heavy Impact Test Theater (HITT), will provide a fully commissioned unique apparatus for the purpose of conducting damaging ice-impact tests on actual vessel hull structures that capture hydrodynamic effects. The present study involves numerical simulations that assist the design work, both for equipment and operations, associated with the HITT facility.

SIMULATION COMPONENTS

The essential simulation components of the HITT apparatus are shown in Figure 1. Figure 2 shows the apparatus in the Ice Tank water environment. The figures illustrate the impacting

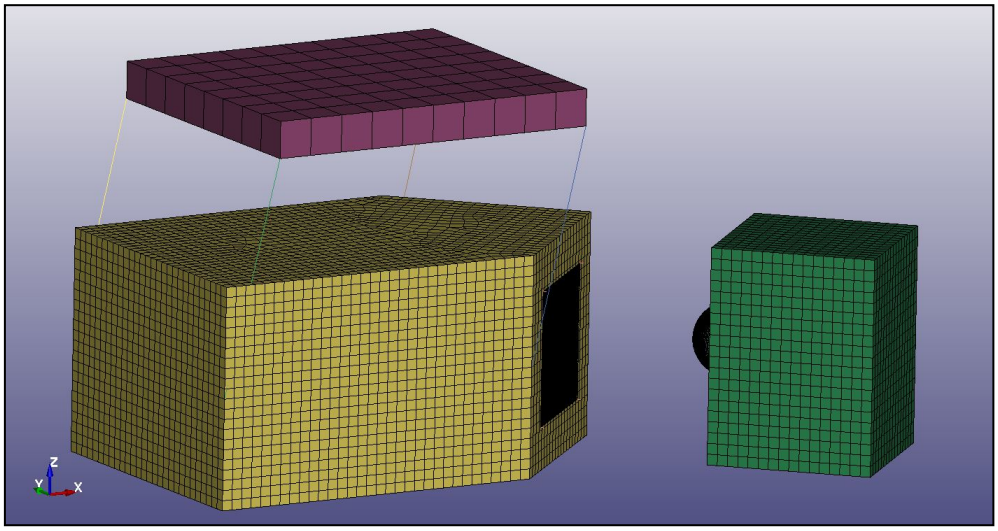

Figure 1. HITT apparatus simulation components: Carriage (purple); Hammer (yellow); Anvil (green); Chains/cables (lines between Carriage and Hammer); Grillage (dark rectangle on Hammer face; Ice (dark hemispherical ice mass on the Anvil). Note that the relative shapes and sizes of most of the components are realistic, whereas the Carriage is simply represented as a thick plate.

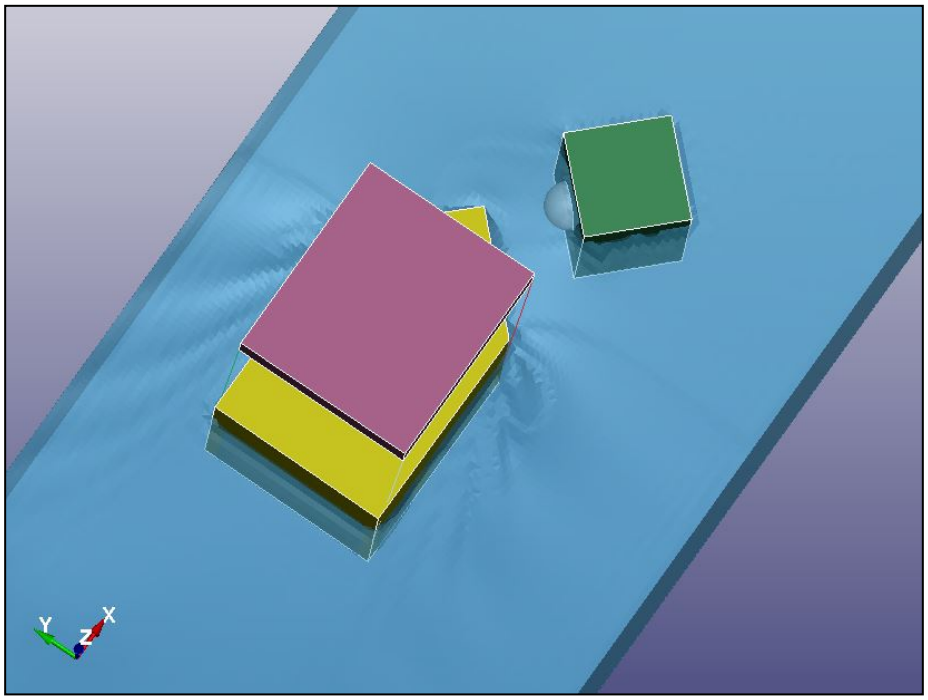

Figure 2. HITT apparatus in the Ice Tank environment just prior to an impact: Carriage (purple); Hammer (yellow); Anvil (green); Chains/cables (lines between Carriage and Hammer); Ice (light blue hemispherical ice mass on the Anvil); Ice Tank water domain (blue, 12 m tank width) with waves associated with the moving Hammer. The Grillage, on the front face of the Hammer, is not visible from this perspective. Note that the relative shapes and sizes of most of the components are realistic, whereas the Carriage is simply represented as a thick plate.

object, known as the Hammer (yellow), supported by four Chains/cables from the Ice Tank Carriage (purple). Also shown is the struck object, known as the Anvil (green), with the hemispherical ice mass attached to one of its sides. In Figure 1 the ship Grillage is the dark rectangular shape on one of the leading faces of the Hammer. Table 1 gives the masses and dimensions of the main components of the simulation. The Grillage is the same as the one used in the earlier study by Gagnon et al. (2018). The Hammer, Carriage, Anvil and Ice consist of solid elements, whereas the Grillage consists of shell elements. The Lagrangian convention was used for all solid structures. The Ice Tank water and internal water masses of the Hammer and Anvil were handled using the ALE convention.

The Hammer (and Anvil) has solid brick elements for its full volume, where the material density is such that the mass of the Hammer hanging on the Carriage by the Chains/cables matches the mass of steel that the actual hollow Hammer has (see Table 1). Occupying the same space of those elements (up to the water line) is the additional water mass that resides inside the Hammer (bounded at its vertical-sided periphery).

A validated ‘crushable foam’ material model (Gagnon and Derradji-Aouat, 2006) was used to characterize the Ice. To do this, LS-Dyna’s material model MAT_63 was used with the following inputs: Density = 870 kg/m3, Young’s Modulus = 9 GPa, Poisson’s Ratio = 0.003, Tensile Stress Cutoff = 800 MPa, and the Yield Strength versus Volumetric Strain curve was essentially the same as that used by Gagnon and Derradji-Aouat (2006).

Table 1. Masses and dimensions of the main simulation components (full-scale).

Component	Mass (kg)	Dimensions Length x Width x Height (m)
Hammer + internal water	12,000 + 54,850	6.64 x 4.0 x 3.0 Hammer 6.64 x 4.0 x 2.433 Water
Anvil + internal water	5,776 + 12,582	2.212 x 2.212 x 2.917 Anvil 2.212 x 2.212 x 2.571 Water
Grillage	245	1.83 x 1.76 x 0.18
Carriage	78,002	---------
Chains/cables	32.4	3.24 Length
Ice Hemisphere	228	1 m radius

Not shown in Figures 1 and 2, are two 'water-mass' entities, one that fills the Hammer up to its water line and the other that similarly fills the Anvil. These water-masses served two important purposes. It was previously found that if the Hammer and Anvil had been treated as full-volume solid masses, numerical 'leakage' of Ice Tank water into their elements occurred in an unpreventable/uncontrollable fashion, which led to unrealistic behaviors in the simulations. This was resolved by deliberately filling the two components with suitable water masses that prevented the entrance of Ice Tank water. In actual HITT experiments both the Hammer and Anvil are flooded with water, which intentionally enhances their effective masses during the impacts, without adding undue weight to the Towing Carriage or to the floor of the Ice Tank, which supports the Anvil while permitting its lateral and rotational movements. The second important function of the 'water-mass' entities is that they can be given artificially high viscosity that ensures that their effective inertia is similar to what it would be inside the Hammer and Anvil where structural 'baffles' will be in place to prevent gross sloshing, i.e. linear and rotational motions of the bulk masses relative to the Hammer and Anvil. That is, the inside water-masses are adequately coupled to the Hammer and Anvil structures so that suitably high loads can be generated during the impacts.

SIMULATION STRATEGY AND RESULTS (FULL-SCALE IMPACT)

Following the methods of Gagnon and Wang (2012), the main large objects that do not interact with anything other than water and air, i.e. the Hammer and the Anvil, are given a large (but adequately refined) mesh size that matches the mesh size of the water and air domains since they have to interact. On the other hand, the Ice and Grillage must be finely meshed, since their interaction volume is much smaller, in order to capture the appropriate behaviors during the impacts. These relatively small and finely meshed objects do not have to interact with the water and air because the main hydrodynamic effects are captured by the interactions of the Hammer and Anvil with the water and air. Furthermore, the deformable properties of the Ice and Grillage do not have to be active until they come into contact with one another, that is, they can be treated as rigid objects until the impacts occur. This is computationally efficient, and LS-Dyna provides the user with the convenient option to run a

simulation and control the properties of objects by setting precise times when their deformable properties become active during a simulation.

An important aspect of the simulation is that a suitable distance must be chosen between the initial location of the Anvil from the starting position of the Carriage/Hammer to allow for a realistic acceleration period of the Carriage/Hammer in order to get up to the designated velocity (1.5 m/s) along the Tank. This also facilitated the generation of a realistic bow wave associated with the Hammer. During this time the Ice and the Grillage were assigned rigid properties. Then, just before contact, the deformable properties of the Ice and the Grillage were switched on. This strategy ensured that the hydrodynamics of the interaction were adequately accounted for and that run times were only as long as necessary (roughly 180 hours using 38 CPU's on a HP Z840 Workstation). Figure 3 shows the velocity time-series data (in the Ice Tank axis direction) of the Carriage and Hammer. Note that the Anvil was constrained up until just prior to the impact, at which point it was free to move in the horizontal plane. Such a strategy, used in actual growler impact experiments (Gagnon, 2004) and earlier HITT simulations (Gagnon et al., 2018), increases the energy associated with the impact and facilitates efficient positioning of the Anvil.

Figure 4 shows the load time series for the Ice impacting the Grillage. The first peak occurs at about 33.2 s and is responsible for the main sliding-load damage that occurs at the roughly-central region of the Grillage (Figure 5). The Anvil and Ice rebound elastically somewhat from the Grillage after the first load peak, without fully losing contact as sliding continues with some slight plastic damage occurring. Eventually the edge of the Grillage plate, which is rigidly constrained (Figure 5, left), is encountered at ~ 33.8 s. This results in a secondary load peak and more plastic damage near the plate edge (Figure 5, left and center). Throughout the interaction, hydrodynamic forces tend to push the Anvil/Ice against the grillage. The maximum Grillage indentation is shown in Figure 5 (right), and the indentation history is shown in Figure 6.

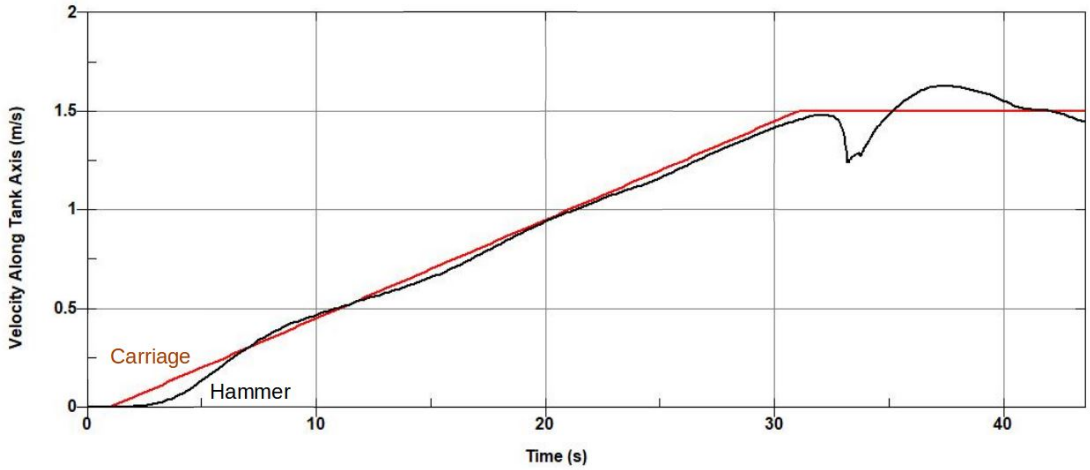

Figure 3. Velocity time series (in the positive X direction, as in Figure 2) for the motions of the Carriage (orange) and Hammer (black) along the Ice Tank axis. The Carriage accelerates uniformly up to the target velocity of 1.5 m/s. The hammer similarly accelerates up to the target velocity while exhibiting some oscillations (diminishing in amplitude) associated with its swinging motion on the Chains/cables. Impact initiates at approximately 33.1 s.

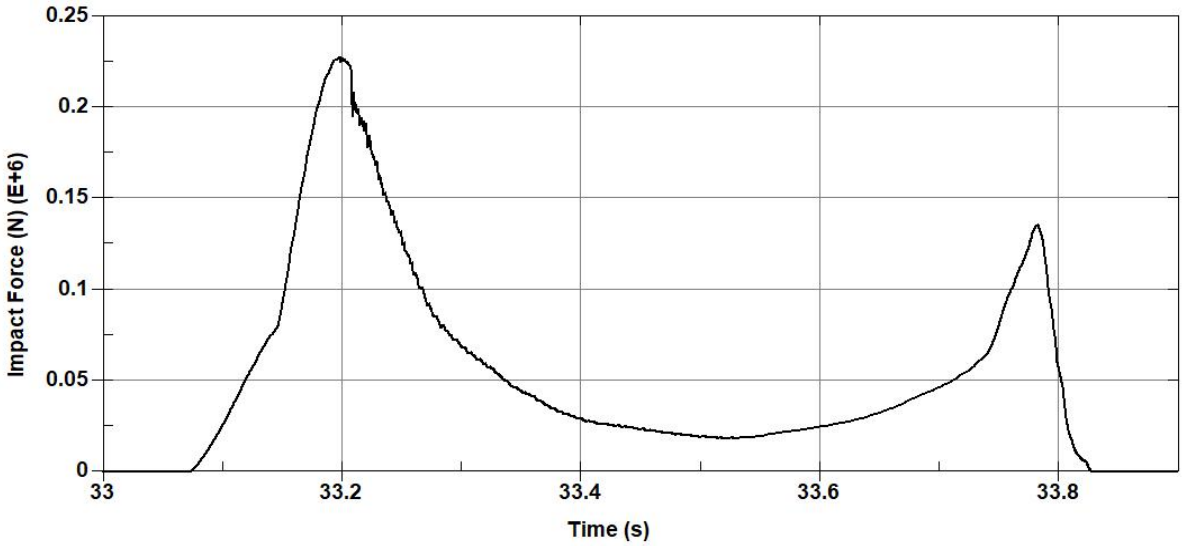

Figure 4. Load time series for the Ice impacting the Grillage. Due to the scenario setup, the data correspond to a glancing-blow sliding load, where the first contact occurs roughly in the center of the grillage between its two stiffeners, generating the first load peak at 33.2 s. The lower-magnitude second peak (at ~ 33.8 s) occurred when the ice contact zone reached the Grillage-plate edge, where the edge was rigidly constrained.

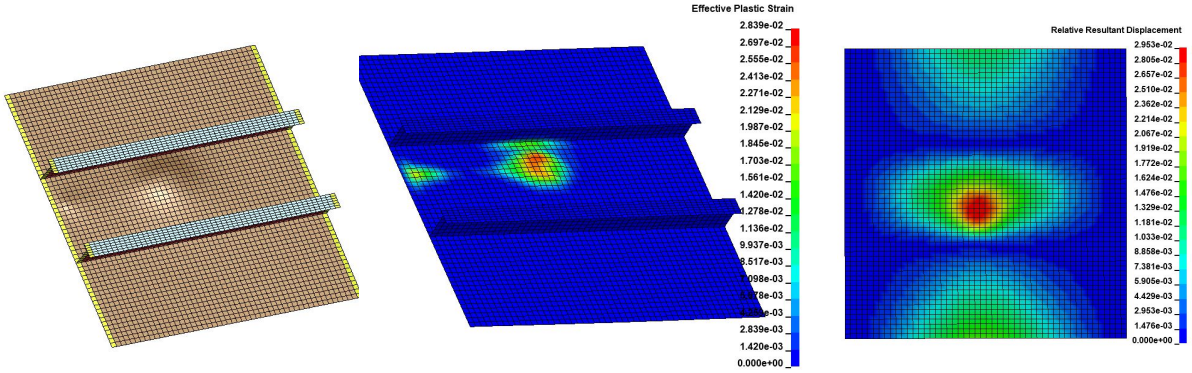

Figure 5. (Left) Light-shaded indented Grillage following impact, with rigid boundary conditions (yellow) on the right and left edges; (Center) Effective plastic strain of the Grillage following impact; (Right) Relative Plate indentation fringes at time of peak load, where the unit on the scale is 'meter'. Note in the left image that an earlier unpublished study showed similar results regardless of whether the boundaries parallel to the stiffeners were fixed or not. Also note that the stiffeners are horizontal in the right image, and the outside of the Grillage is facing the viewer.

Figure 6 shows that the peak indentation (~ 29 mm) occurs at about 33.2 s, and the residual plastic deformation (~ 20 mm) is evident at around 33.5 s. These values are similar to those obtained by Gagnon et al. (2018) for the same Grillage (~ 31 mm and ~ 24 mm respectively), where in that case a Hammer with similar mass was constrained to move at a constant speed (without surge, sway, yaw or heave) during the impact. Another difference was that the grillage was rigidly constrained at all four side edges.

Figures 7 and 8 show the lateral displacement of the Hammer and the consequent lateral force

applied to the Carriage during the simulation. Note that there is a significant degree of lateral sway, and associated lateral force, starting at around 19 s, well before the impact occurs at about 33.1 s. This we attribute to the fact that the Carriage and Hammer were not centered in the Ice Tank water domain during the simulation (Figure 2) and there was likely more bow-wave interaction with the closer Ice Tank wall on the port side of the Hammer. This explanation is further supported by half-scale simulations of tests conducted in NRC's Towing Tank that did not involve impact (discussed below). In those simulations, and the actual experiments, the Carriage and Hammer were centered in the tank, and there was no significant lateral sway of the Hammer.

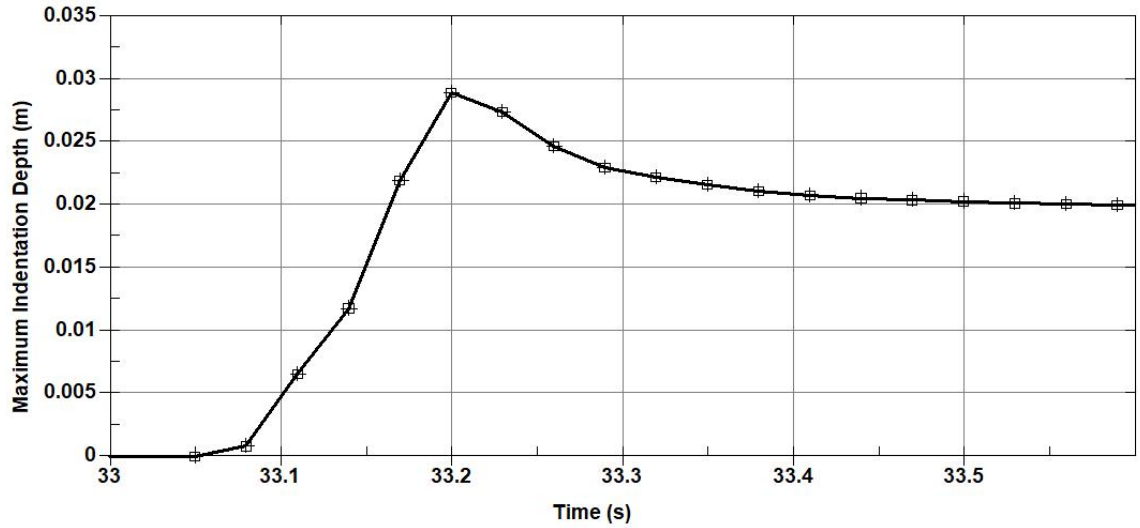

Figure 6. Maximum indentation depth time series for the Ice impacting the Grillage. The peak value appears to be at 33.2 s, but is probably slightly after that time because the marginal data-point frequency appears to have 'clipped' the peak somewhat. Following the peak load, there is some elastic rebound until the residual plastic indentation is evident at about 33.5 s.

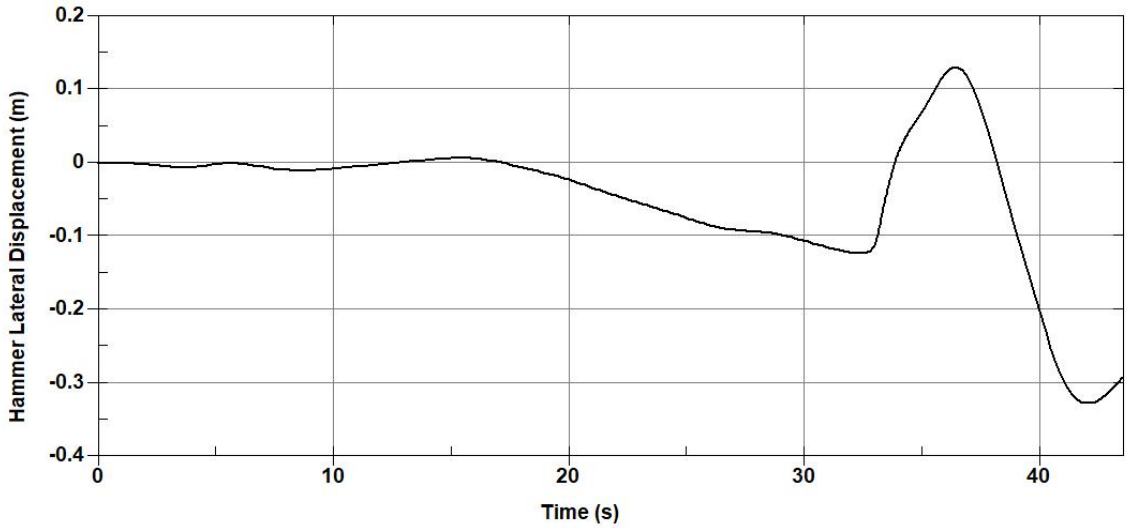

Figure 7. Time series of the lateral displacement of the Hammer (in the positive Y direction, as in Figure 2) during the simulation.

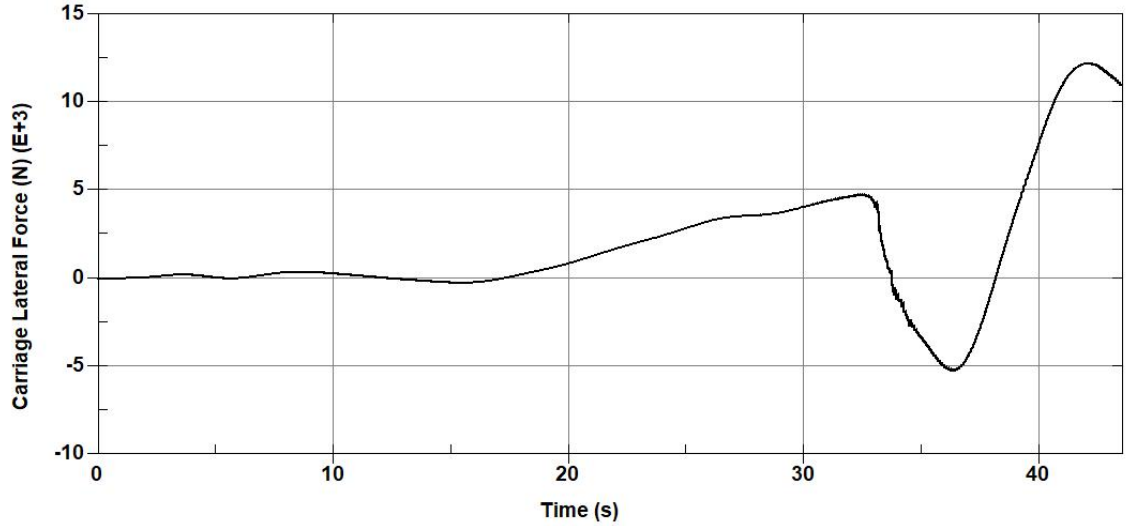

Figure 8. Time series of the lateral force (in the negative Y direction, as in Figure 2) on the Carriage due to lateral motion of the Hammer during the simulation.

Because the impact occurred on the front end of the Hammer, a degree of yaw was also imparted to it, as shown in Figure 9. Note that the yaw angle is most pronounced following the initiation of ice contact that occurs at ~33.1 s.

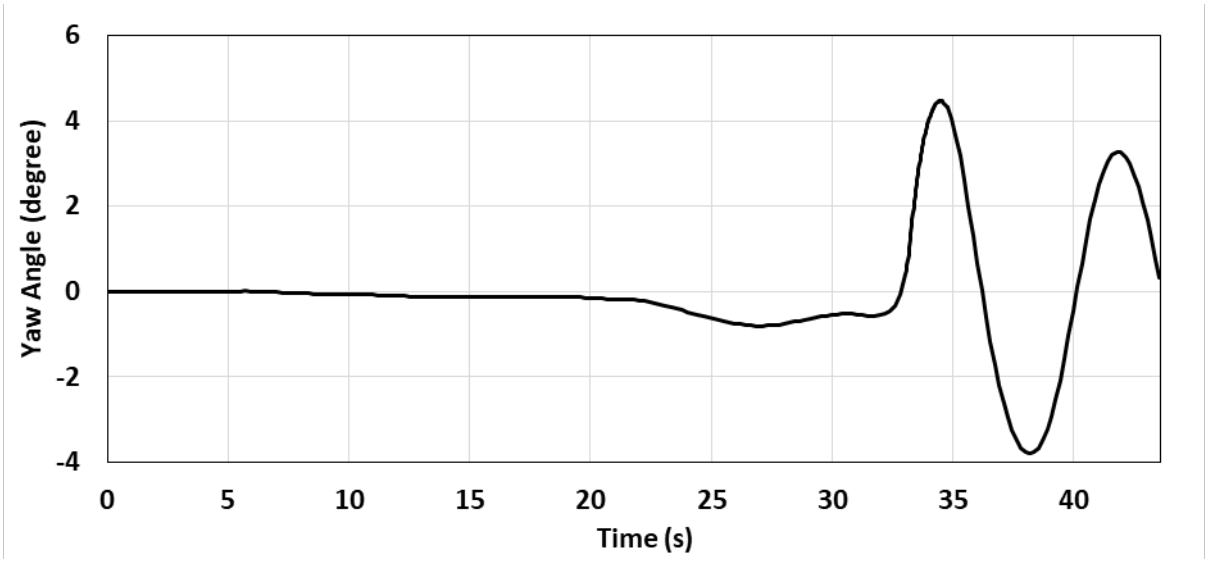

Figure 9. Time series of the yaw angle of the Hammer. The yaw angle is with respect to the X-axis in the positive X-Y plane of the Ice Tank, as in Figure 2.

HALF-SCALE TOW TANK TEST DATA COMPARISON WITH A SIMULATION

Figure 10 shows relative-motion data of the Carriage and Hammer from a half-scale non-impact experiment conducted in the Tow Tank, and from a corresponding numerical simulation using the same test parameters. The main test components are the Carriage, the

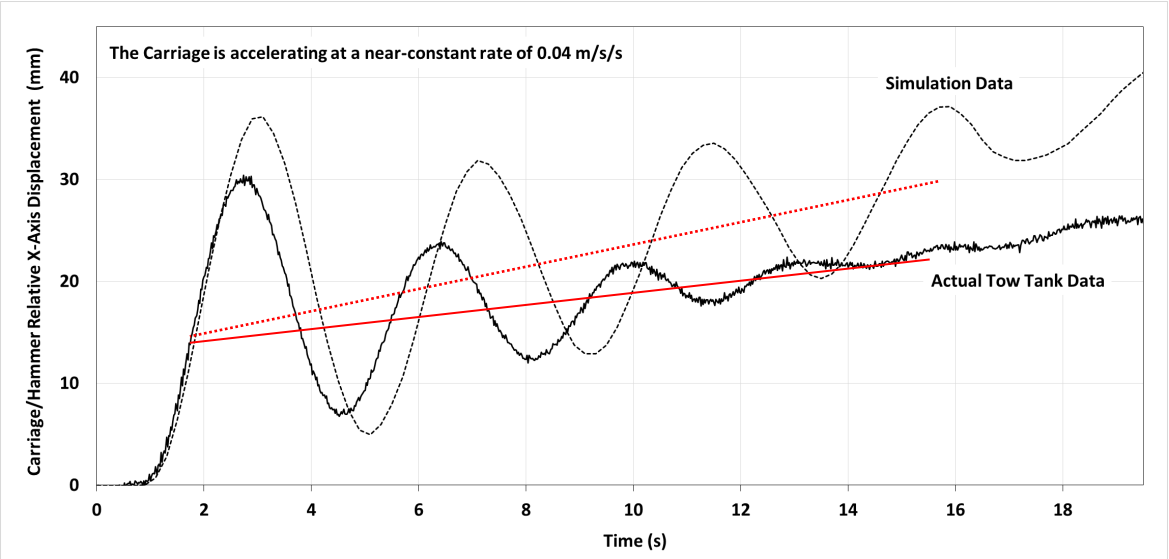

Figure 10. Time series of the relative displacement of the Carriage and Hammer for a Tow Tank experiment and a simulation of the test using the same parameters. In this comparison of the experimental and simulated data only the first 20 s of the actual Tow Tank data are used because the simulation had not run to completion at the time this paper was submitted. The axis of motion (the positive X-axis) is along the Tow Tank length, as in Figure 2.

Hammer and the Chains/cables (similar to the respective components in Figures 1 and 2). The study was intended to investigate hydrodynamic aspects of the equipment behaviors during HITT experiments, and to validate the simulations. In this test scenario the Carriage accelerates at a constant acceleration of ~ 0.04 m/s^2 until it reaches the target speed of 1.06 m/s, where it then continues at that speed for a short period and then decelerates, at the same rate as the acceleration phase, until coming to a stop. Here we show only a portion of the acceleration phase to illustrate the key observations from the test and simulation. By determining the relative displacement of the Carriage and Hammer in the Tank-axis direction (i.e. the X-axis), one can easily determine the angle on the Chains/cables, from which loads in the X and Z (vertical) directions can be calculated, since the axial loads on the Chains/cables were recorded in both the experiment and the simulation.

We first note that both records show oscillations in the relative displacement, which is due to a certain degree of swinging motion of the Hammer on the Chains/cables that are connected to the Carriage. We also note that in the 0-5 s period that the amplitude of the simulation oscillations is somewhat greater than that of the Tow Tank data. Similarly, the period of the oscillations is greater for the simulation data. These characteristics we attribute, for the most part, to the fact that the experimental Hammer had a 22% portion of its bottom open, whereas the simulation Hammer had its bottom completely closed. Consequently, a certain amount of the water inside the Hammer in the experiment was not subject to the same degree of acceleration as the water filling the Hammer in the simulation. That is, the ‘effective mass’ of the Hammer and inner water in the simulation was greater than that in the Tow Tank experiment. Hence, given the same spring-like restoring-force mechanisms in both cases, the amplitude and period of the Hammer oscillations in the simulation were greater than that in the experiment. We further note that the more pronounced damping of the oscillations in the experimental data may have resulted from energy absorbed by circulation of water inside the

experiment Hammer, due to the open portion of its bottom. Also, we note that both data plots generally increase in time, due to the increase of hydrodynamic forces on the Hammer with increasing speed. Finally, if we draw straight lines (Figure 10, red lines) through the estimated 'average' of the oscillations in both cases, we observe that they approximately intersect at the 14 mm relative-displacement amount at the early stage of the acceleration of the Carriage and Hammer, where the speed is low and the damping effect just mentioned is not so pronounced. This corresponds to an angle of about 0.8^o on the Chains/cables, which translates to a force in the X direction of about 500 N since the vertical component of the axial Chain/cable load, associated with the mass of the steel in the Hammer, is 35.4 kN. Not surprisingly, a 500 N load applied to the Hammer and its inner water mass (~ 10,614 kg combined mass) results in an acceleration of ~ 0.047 m/s^2. The fact that the two straight lines that were drawn diverge as the test and simulation progress in time we attribute, to some extent at least, to the Bernoulli effect, whereby the Hammer bottom in the Tow Tank experiment (that is partially open), moves over relatively stationary Tank water that creates a reduction in hydraulic pressure inside the Hammer, and consequent lowering of the water level inside the Hammer. The effect would be more pronounced as the Hammer speed increases, that is, the effective mass of the Hammer and its inner water decreases in the Tow Tank experiment, and consequently a diminishing force is required to maintain its nominal acceleration. While this may not fully explain the degree of divergence of the lines that were drawn, it may at least be a contributing factor.

AN EXAMPLE OF SIMULATION USEFULNESS

We now briefly mention an example of how simulations of this type can inform the design and operational-procedure aspects of the HITT facility. One of the purposes of this study was to assess the effect of lateral motion of the Hammer due to the Ice impacts. While the impulsive load lasts for a short duration (< 1.0 s, as in Figure 4) and generates lesser amounts of immediate sway and associated load during that time, the kinetic energy (i.e. lateral velocity) imparted to the Hammer leads to more substantial sway and lateral load some seconds later (Figures 7 and 8). The range of generated lateral loading, from about -5 kN to 12 kN, needs to be considered in terms of potential effects on the rails that the Carriage rides on. Mitigating strategies will be necessary, such as giving lateral rolling capability to the frame on the Carriage that the Hammer Chains/cables are attached to, thereby removing sway-induced side loads.

CONCLUSIONS

In previous studies of the planned HITT apparatus, motions of the Hammer were prescribed and constrained, thereby avoiding the inclusion of the towing carriage and means of attachment. That preliminary numerical approach, while useful at the time, has now been upgraded to the full intended realistic scenario where the Hammer is supported and towed by the Ice Tank Carriage through the use of flexible Chains/cables that give the Hammer all the degrees of freedom it will have in the actual experiments, i.e. surge, sway, yaw and heave. This enhancement gives the simulations enough sophistication to be useful as aides in the HITT design process, and development of related experimental procedures.

We recognize that there are size limitations to what can be done in the lab environment with respect to whole-ship interaction with ice masses. However, our main purpose is to test the

reliability of the simulations when compared to actual grillages (even if limited in size) sustaining damage due to ice impacts in the HITT facility. Positive reliability results in those circumstances lead to confidence in past and future simulation results of whole ships colliding with floating ice masses.

ACKNOWLEDGEMENTS

The authors are grateful to DRDC and the Office of Naval Research (ONR) for providing the resources to conduct this work, and to NRC for its long-standing commitment to ice-ship and ice-structure interaction studies.

REFERENCES

Daley, C., Hermanski, G., Pavic, M., Hussein, A., 2007. Ultimate strength of frames and grillages subject to lateral loads—an experimental study. 10th International Symposium on practical design of ships and other floating structures. Houston, Texas.

Gagnon, R., 2004. Analysis of Laboratory Growler Impact Tests. Cold Regions Science and Technology, 39, 1-17.

Gagnon, R.E. and Derradji-Aouat, A., 2006. First Results of Numerical Simulations of Bergy Bit Collisions with the CCGS Terry Fox Icebreaker. Proceedings of IAHR, Sapporo, Japan, Vol. 2, 9-16.

Gagnon, R.E. and Wang, J., 2012. Numerical Simulations of a Tanker Collision with a Bergy Bit Incorporating Hydrodynamics, a Validated Ice Model and Damage to the Vessel. Cold Regions Science and Technology 81, 26-35.

Gagnon, R., Quinton, B., Mackay, J., 2018. Heavy Impact Test Site (HITS) Simulations. Proceedings of the 24th IAHR International Symposium on Ice. Vladivostok, Russia, June 4 to 9, 2018.

Kõrgesaar, M., Kujala, P., Romanoff, J., 2018. Load carrying capacity of ice-strengthened frames under idealized ice load and boundary conditions. Marine Structures 58: 18-30.